

Research Article

Photocatalytic Activity of Green Construction TiO₂ Nanoparticles from *Phyllanthus niruri* Leaf Extract

Annin K. Shimi,¹ Saikh Mohammad Wabaidur,² Masoom Raza Siddiqui,² Md Ataul Islam,³ Kantilal Pitamber Rane,⁴ and T. S. Arul Jeevan⁵

¹Department of Physics, Manonmaniam Sundaranar University, Tirunelveli, Tamil Nadu 627012, India

²Department of Chemistry, College of Science, King Saud University, Riyadh 11451, Saudi Arabia

³Division of Pharmacy and Optometry, School of Health Sciences, Faculty of Biology, Medicine and Health, University of Manchester, Manchester, UK

⁴KCE College of Engineering and Management, Jalgaon, Maharashtra 425001, India

⁵Department of Chemistry College of Natural and Computational Sciences, Mizan Tepi University, Tepi, Ethiopia

Correspondence should be addressed to T. S. Arul Jeevan; jejeevan@mtu.edu.et

Received 29 December 2021; Revised 11 March 2022; Accepted 25 May 2022; Published 22 June 2022

Academic Editor: Awais Ahmed

Copyright © 2022 Annin K. Shimi et al. This is an open access article distributed under the Creative Commons Attribution License, which permits unrestricted use, distribution, and reproduction in any medium, provided the original work is properly cited.

The present research work reports the facile and green synthesis of TiO₂ nanoparticles from *Phyllanthus niruri* leaf extract using the coprecipitation method. The plant biomolecules were responsible for the nanoproduction and exhibited reduction and stabilization activity. The green synthesized TiO₂ nanoparticles were analyzed in various characterization methods. The crystalline size (23 nm) and anatase phase of TiO₂ nanoparticles were analyzed from X-ray diffraction study. The reduction and stabilization response functional group of TiO₂ nanoparticles was studied from FTIR analysis. The optical properties of TiO₂ nanoparticles were constructed from the UV-DRS technique, and their calculated bandgap is 3.16 eV. The spherical morphology and their existing materials were identified using FESEM with EDX. The catalytic activity of TiO₂ nanoparticles was examined against methylene blue dye under ultraviolet and visible light irradiation. It was detected that ultraviolet irradiation showed higher photocatalytic activity than visible light irradiation. In addition, visible light irradiation provides the above 90 percentage degradation of methylene blue dye. Hence, TiO₂ nanoparticles were proposed as a potential catalyst of photocatalytic dye degradation application and water remediation activities.

1. Introduction

Nanoscience is one of the most widely used and effective fields of research in scientific discovery. Nanotechnology has recently become a highly advanced technology with intra- and interstudy spanning chemistry, physics, biology, material science, and medicine. The production of nanometer-sized materials of various morphologies and sizes, as well as monodispersion, is an important field of research in nanoscience [1, 2]. Nanoparticles of varying sizes, shapes, and controlled disparity are synthesized by many researchers. Catalysis, optical, electric, and magnetic aspects; diagnostics; biological probes; and display devices are among the applications for metal nanoparticles [3].

The synthesis of metal and metal oxide nanoparticles is an existing field of material chemistry that has piqued interest due to applications in a wide range of fields, including air and water purification, medicine, antimicrobials, information technology, photocatalytic, antimicrobial, energy reservoirs, and biosensors [4]. Nanomaterial synthesis methods are divided into physical and chemical processes due to their enormous surface area. These procedures, however, are not ideal for medical and biological applications due to their environmental hazards. As a consequence, researchers are opting for a green synthesis method to synthesize nanomaterials although it is efficient, environmentally friendly, and cost effective [5, 6]. Green synthesis is an exciting material science approach [7–9]. Plants provide a better platform

for nanoparticle manufacturing since they do not contain hazardous compounds and provide natural capping agents [10]. Numerous organic substances are widespread in nature extracts including amino acids, proteins, polysaccharides, alkaloids, flavonoids, and phenolic compounds [11–13]. TiO₂ has become extremely prevalent in a broad spectrum of applications [14–24]. TiO₂ is an excellent material for photocatalysis and biomaterial creation [25]. Titania's biocompatibility makes it suitable for use in bone tissue engineering for bone regeneration and healing [26]. TiO₂ is a powerful catalyst that may be used to remove a variety of contaminants from the environment and has been shown to clean water and surfaces [26–34]. The *Phyllanthus* genus is one of the most prominent groupings of plants traded in India as a raw herbal medication [35]. The *Phyllanthus* genus, which belongs to the *Euphorbiaceae* family, contains over 1000 species that are found on tropical and subtropical continents like America, Africa, Australia, and Asia. The *Phyllanthus* genus is widely applicable in the human medical system [35–39]. *Phyllanthus niruri* has been used in traditional medicine to treat lung and skin-related diseases. The presence of various biologically active substances serves an impeccable role in the reduction, capping, and stabilization processes. These plant compounds reduced the toxicity level during the production of nanophase materials. Moreover, the plant derivatives obtained various bioactive elements that can be used in antibacterial, antifungal, and diabetic-related applications [39–47]. The bioreduction compounds of lignin, saponins, and flavonoids give the chemical-free zero-valent atom and provoke the stabilization process. In addition, these biocompounds increased microbial resistivity and are highly appreciable in liver-related diseases. The present work investigates the nanoproduction of TiO₂ nanoparticles using *Phyllanthus niruri* leaf extract. The structural, optical, and morphological entities of the synthesized nanoparticles were investigated. In addition, the photocatalytic activity of the synthesized nanoparticles was observed from ultraviolet and visible light irradiation.

2. Experimental

2.1. Materials. The titanium tetra isopropoxide (TTIP) (Sigma-Aldrich, AR grade, purity > 99 percent) was used to synthesize the TiO₂ nanoparticles. Fresh leaves of *Phyllanthus niruri* were collected from Tirunelveli, and their extract was used as a bioreductant. The methylene blue dye was purchased from HiMedia. There are no extra chemicals were used for the purification and synthesis process.

2.2. Green Synthesis of TiO₂ NPs. The *Phyllanthus niruri* leaf extract and 0.1 M TTIP solutions were used in the green synthesis of TiO₂ nanoparticles. 0.1 M TTIP solution was poured into 90 mL leaf extract under magnetic stirring. The stirring and biomolecules of the leaf extract have modified the color into white and produced precipitation. The white precipitation was centrifuged for 12000 rpm for 15 minutes two times. The obtained pellets were filtered with Whatman no. 1 filter paper and kept in an oven for 200°C at 3 hrs. Finally, the white TiO₂ nanoparticles are character-

ized by various analyses. The formation of TiO₂ is depicted in Scheme 1.

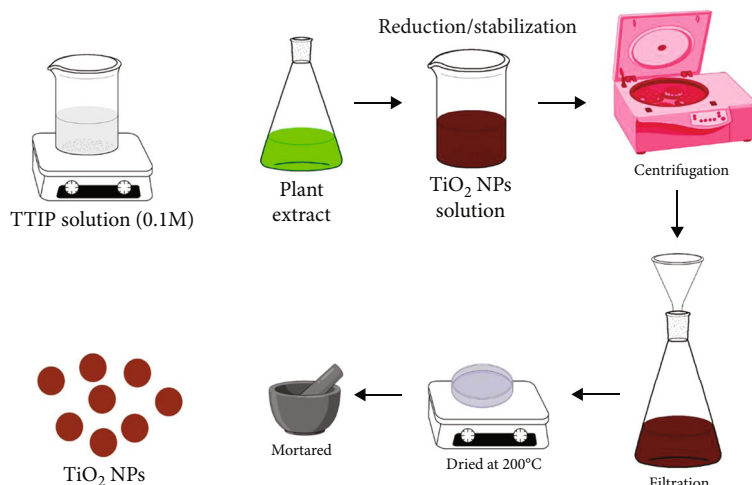
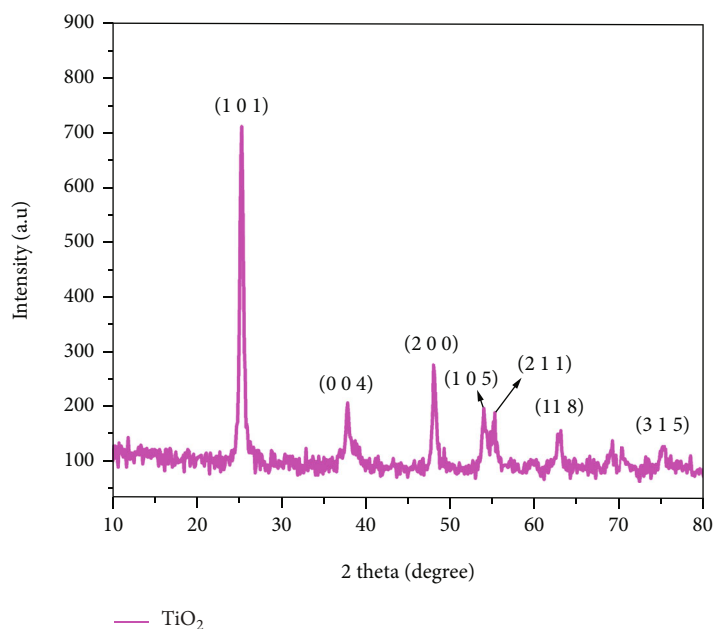
2.3. Characterization. The synthesized TiO₂ nanoparticles were evaluated by structural, optical, and morphological analyses. The crystalline property of TiO₂ nanoparticles was observed from the X-ray diffractometer (XRD) (PANalytical X-ray diffractometer, Cu-K α radiation = 0.154 nm, angle 10°–80° and 40 kV/15 mA). The optical property of TiO₂ nanoparticles was captured from the UV Shimadzu 2700 UV-DRS spectrophotometer. The functional group and formed TiO₂ nanoparticles were recorded from the FT-IR (PerkinElmer, 400–4000 cm⁻¹, USA). The morphological entity was observed from scanning electron microscopy (HRSEM-SEM, Carl Zeiss, Germany) coupled with material identification energy-dispersive X-ray spectroscopy (EDX).

2.4. Photocatalytic Activity. The photocatalyst of TiO₂ nanoparticles was performed against visible and UV light irradiation to determine the photocatalytic MB dye degradation. The light source is an important key factor to modify the rate of degradation to degrade the organic pollutants. The 10 ppm MB (100 mL) dye solution was inoculated with a 10 mg photocatalyst. After that, the combined solution was kept in dark condition to attain the adsorption-desorption equilibrium level. Finally, the mixed solution was placed in UV and visible light circumstances. The irradiated samples were withdrawn (5 mL) in a regular interval (30 minutes) to measure the degradation efficacy of TiO₂ nanoparticles. The photocatalytic dye degradation efficacy was observed from the following equation: dye degradation efficiency = $C - C_1/C$, where C is the initial dye absorbance at time = 0, C_1 is the dye absorbance with light at time = 30 min, and t is the time.

3. Results and Discussion

3.1. X-Ray Diffraction (XRD). The X-ray diffraction pattern of the green synthesized TiO₂ nanoparticles is shown in Figure 1. The structural, crystallite size and material phases were identified from X-ray diffraction. The obtained peaks are 25.27° (1 0 1), 37.86° (0 0 4), 48.23° (2 0 0), 54.31° (1 0 5), 55.09° (2 1 1), 62.62° (1 1 8), and 75.21° (2 1 5) compared with those of the standard JCPDS card no. 78-2486 [48, 49]. The anatase phase of TiO₂ nanoparticles exhibits enhanced catalytic activity than the rutile and brookite phases. The photocatalyst TiO₂ nanoparticle crystallite size was calculated from the Debye Scherrer formula, and their calculated value is 23 nm in (1 0 1) plane at a high-intensity peak. The lowest crystallite size demonstrates the large surface area and outstanding photocatalytic activity of the synthesized materials.

3.2. FTIR Analysis. The plant active functional groups of the TiO₂ nanoparticles were analyzed by FTIR spectrum and displayed in Figure 2. The broad peak at 4000–3500 cm⁻¹ specifically at 3420 cm⁻¹ belongs to hydroxyl groups of O–H stretching vibration [50]. The band at 2923 cm⁻¹ is attributed to C–H vibrations. The C–H vibrations are restricting

SCHEME 1: Synthesis formation of TiO_2 nanoparticles.FIGURE 1: XRD diffraction pattern of green synthesized TiO_2 NPs.

the phase changes and promote the organic precipitation in synthesis time. Another prominent peak of TiO_2 nanoparticles is located at 1627 cm^{-1} , which can be ascribed to $\text{C}=\text{C}$ which came from plant carbon molecules. The carbon molecules are associated with hydrogen and oxygen from the source materials. The carbon association produces the $-\text{C}-\text{O}$ stretching and $-\text{C}-\text{H}$ bending to the source precursors [50–53]. These compounds come from the plant extract biomolecules which can control the growth of the particles and reduction/stabilization activity. The peak at 720 cm^{-1} is attributed to the $\text{Ti}-\text{O}$ stretching bands. The stretching modes of $\text{Ti}-\text{O}-\text{Ti}$ all are observed at $500\text{--}700\text{ cm}^{-1}$ [54]. The plant bioderivatives produce the nonvalent atoms through the flavonoids, saponins, and lignin. These plant derivatives are responsible for metal and oxygen bond for-

mation. The formed metal and oxygen elements were stabilized from plant derivatives.

3.3. UV-DRS Analysis. The optical properties of the TiO_2 nanoparticles were performed from the UV-DRS technique. The DRS spectrum is shown in Figure 3(a) which can indicate the optical reliability of the TiO_2 nanoparticles in the UV region at 390 nm. The optical transformations and their defects were determined the bandgap of the materials. There is no adsorption edge involved in the visible region which can denote the highest photonic energy. The optical bandgap values are calculated from Tauc eqn. The calculated bandgap value shows the relationship between the incident photon energy of semiconductors and absorption coefficient: $ahv = A(hv - E_g)^n$, where α is the absorption coefficient, v is

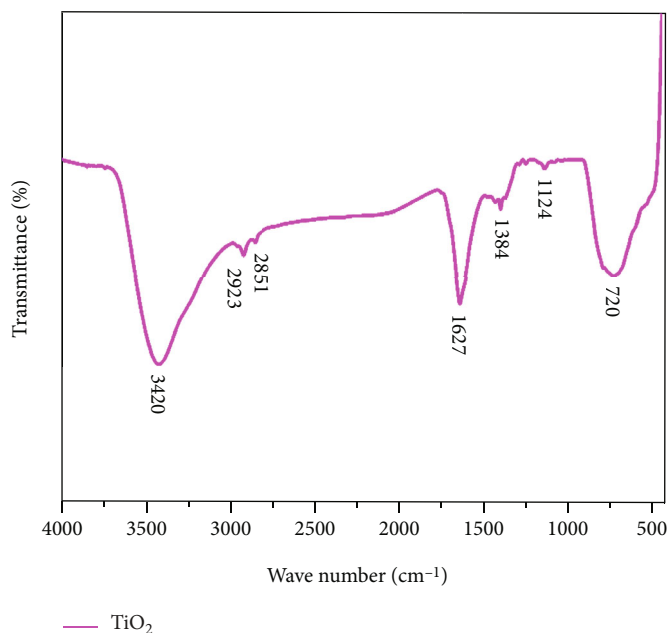


FIGURE 2: FTIR spectrum of green synthesized TiO_2 NPs.

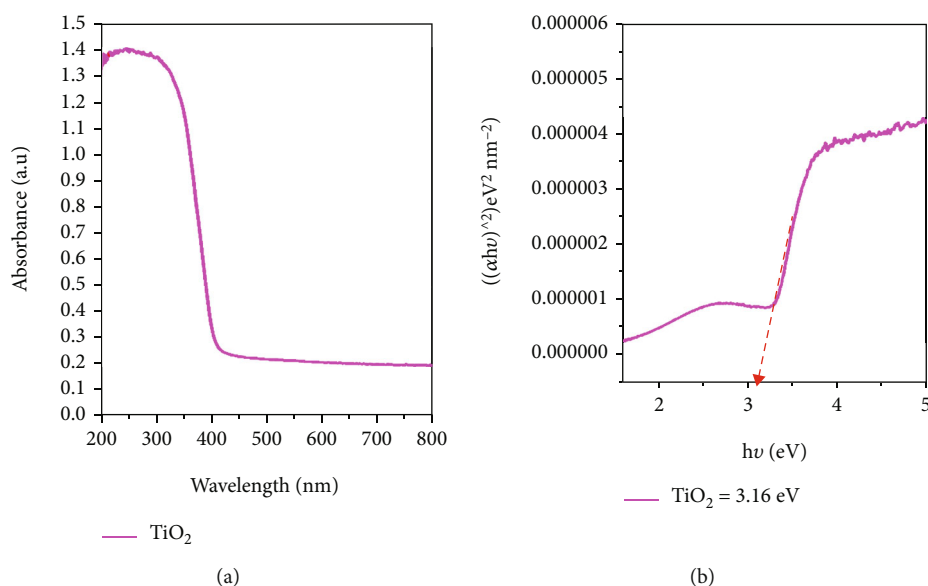
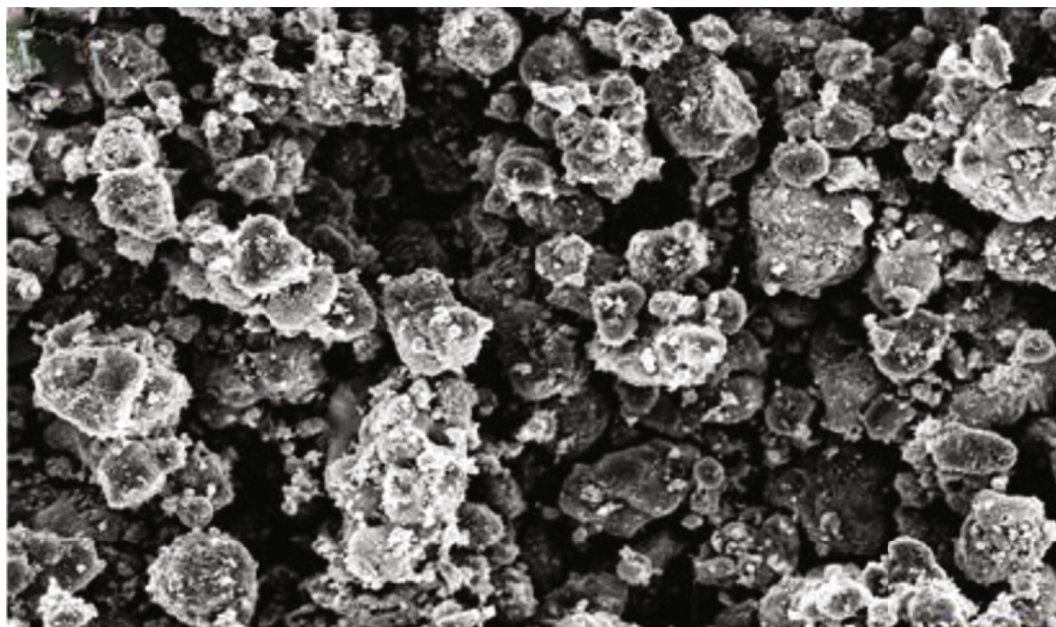


FIGURE 3: (a) UV-DRS absorption spectrum and (b) bandgap energy spectrum of green synthesized TiO_2 nanoparticles.

the frequency, E_g is the Bandgap, and n is the $1/2$ direct bandgap semiconductor. The obtained band gap is 3.16 eV. The wide bandgap of TiO_2 nanoparticles exhibited the charge carrier formation and liberation in the photocatalytic activity [55, 56].

3.4. FESEM with EDX. Figure 4 shows the surface morphological and elemental analysis of green synthesized TiO_2 nanoparticles. FESEM images represent the spherical morphology with even distribution on the surface. The formed spherical shape and their smaller size particles accelerate the free radical formation. The existing plant biomolecules occupied the surface which gives the agglomerations and

large grain size particles. The existing plant molecules derived the irregular distribution of the TiO_2 nanoparticles. The spherical shape is a more benefit able shape in catalytic activity than other shapes due to their large surface area [57–60]. The EDX spectrum displays the Ti and O element existence over the surface. The remaining small peaks exhibit the plant molecules which was well explained in FTIR analysis. The elemental percentages were displayed in Figure 4(d). The Ti elements occupied the major places in synthesized TiO_2 nanoparticles. The FE-SEM morphology images showed the spherical and semispherical shapes of the TiO_2 nanoparticles. The spherical shape occupied the major area of the TiO_2 nanoparticles which are attached to

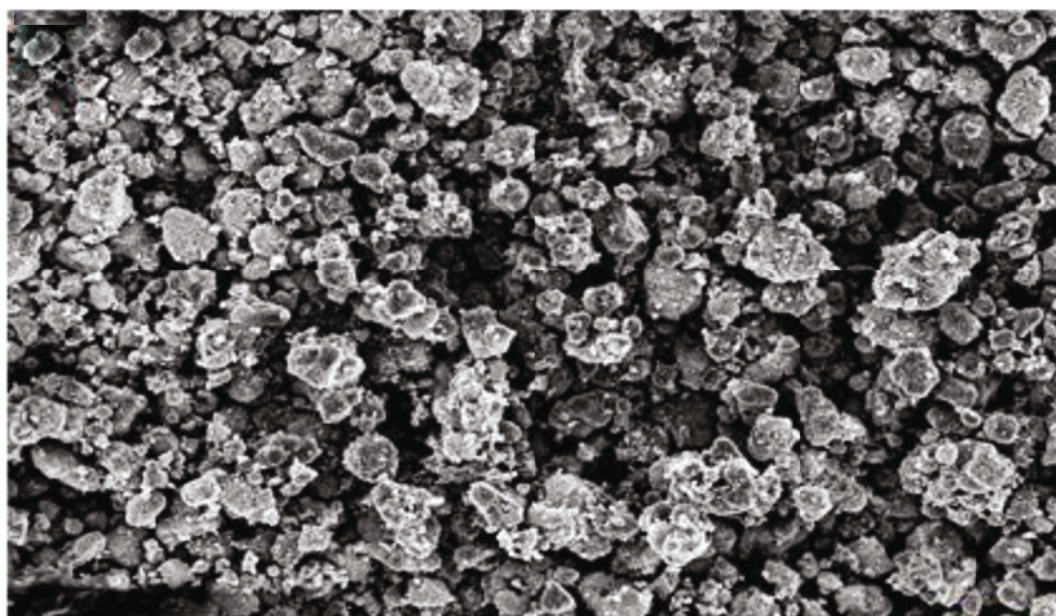


1 μm

EHT = 5.00 KV
WD = 5.6 mm

Signal A = Inlens
Mag = 10.00 KX

(a)



2 μm

EHT = 5.00 KV
WD = 5.6 mm

Signal A = Inlens
Mag = 5.00 KX

(b)

FIGURE 4: Continued.

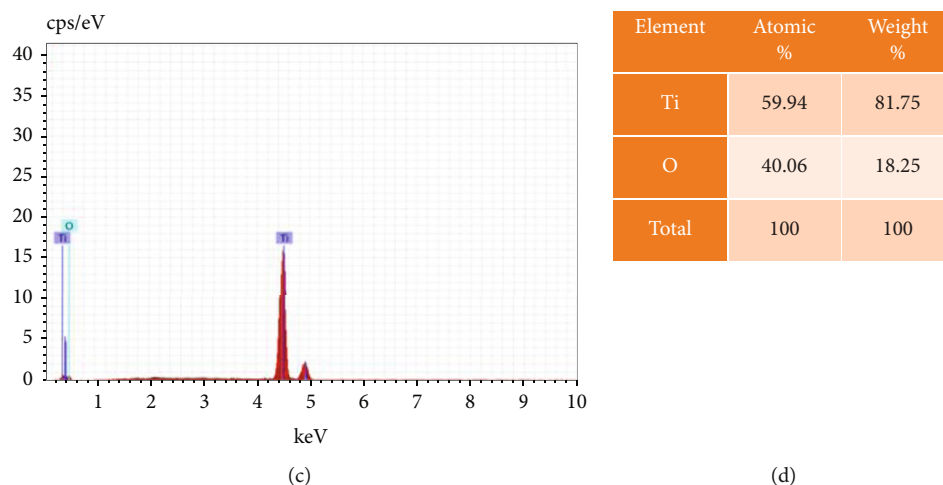


FIGURE 4: (a, b) FESEM images, (c) EDX spectrum, and (d) EDX table of green synthesized TiO_2 nanoparticles.

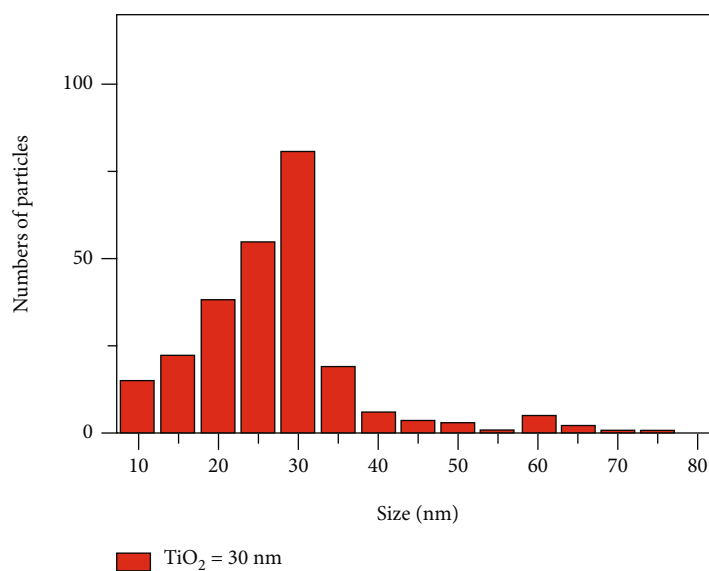


FIGURE 5: Histogram of green synthesized TiO_2 nanoparticles.

it shown as larger grain size particles due to their plant derivatives. The excessive plant compounds construct the layer over the TiO_2 surface and merged the two particles. Therefore, it shows semispherical and spherical shapes. The distribution of the TiO_2 nanoparticles was calculated from ImageJ software, and their values are displayed in Figure 5.

3.5. Photocatalytic Activity. The green synthesized TiO_2 nanoparticles against methylene blue dye under different light sources are shown in Figures 6(a) and 6(b). The visible light irradiation slowly increased the degradation rate due to the reactive sites of the catalyst. Above 60 minutes of visible light irradiation exhibits the higher degradation because of their OH radicals which provokes the oxidation of the dye molecules [61, 62]. The plant biomolecules sustained the electron-hole pair recombination which derived strong oxi-

dation and reduction of dye molecules over the catalyst. This process takes 60 minutes to 90 minutes with the migration of electrons and holes of the concern bands. The ultraviolet irradiation exhibits the vigorous degradation than visible light irradiation due to their OH radicals [16–23]. The ultraviolet light provokes the electron mobilization and evoked the electron-hole pair which promotes better degradation efficiency. The 30-minute ultraviolet light irradiation of TiO_2 nanoparticles exhibited above 80% degradation. The ultraviolet irradiation (98.2%) of TiO_2 nanoparticles showed enhanced degradation efficiency than visible light irradiation (94.42%) (Figure 7(a)). The photocatalyst efficiency was calculated from the C/C_0 spectrum (Figure 7(b)) The degradation efficiency is dependent on a light source, catalyst dosage, pH, and dye concentration [63]. TiO_2 nanoparticles are extensively used in photocatalytic activity due to their wide bandgap and e-h pair restriction property. The anatase

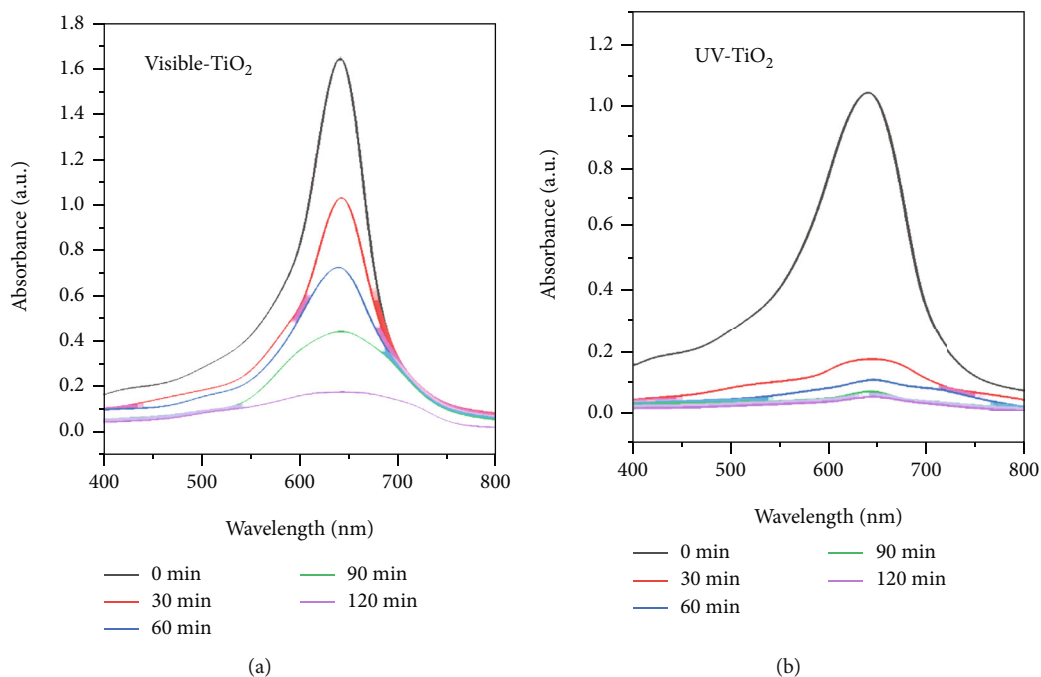


FIGURE 6: Photocatalytic degradation spectrum of the green synthesized TiO₂ nanoparticles.

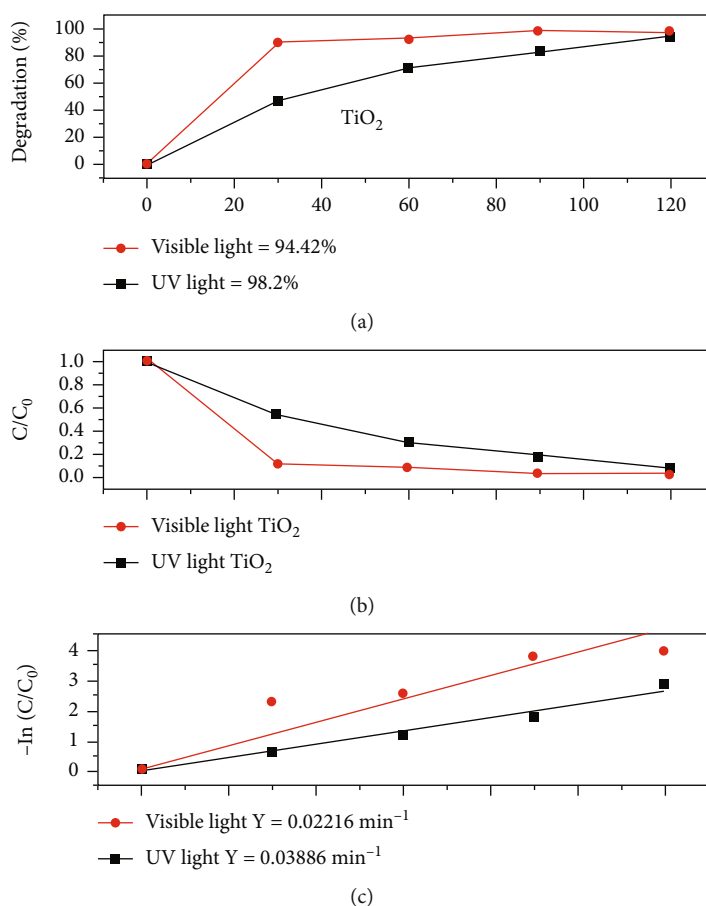
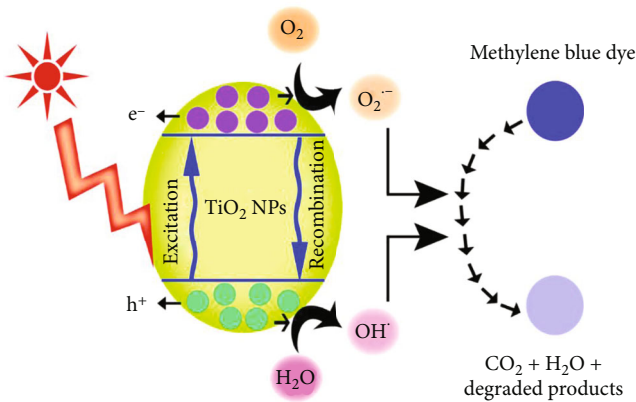


FIGURE 7: (a) Degradation efficacy, (b) C/C₀ absorption rate, and (c) photocatalytic degradation kinetics study of the green synthesized TiO₂ nanoparticles.

TABLE 1: Photocatalytic MB degradation of TiO₂ nanoparticles.

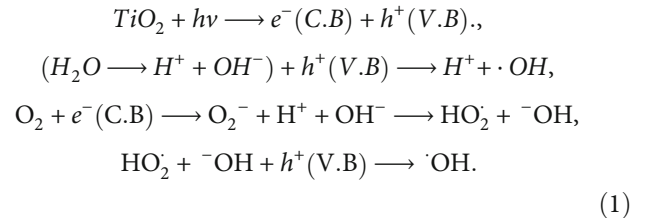
S. no	Nanomaterial	Time (min)	Source	Degradation percentage	References
1	TiO ₂	120	UV-Vis	89	[70]
2	TiO ₂	240	UV-Vis	70	[71]
3	TiO ₂	60	UV-Vis	76	[72]
4	TiO ₂	90	Solar light	90	[73]
5	Co/TiO ₂	150	UV-irradiation	80	[64]
6	Mn-TiO ₂	240	Visible light	88	[65]
7	TiO ₂	60	UV	72.4	[66]
8	TiO ₂	60	UV-Vis	90.4	[67]
9	TiO ₂ /PET	10	UV-vis	88	[74]
10	TiO ₂	120	UV	98.2	Present work
11	TiO ₂	120	Visible light	94.4	Present work

FIGURE 8: Photocatalytic degradation mechanism of green synthesized TiO₂ nanoparticles.

TiO₂ nanoparticles exhibited a wide bandgap (3.16 eV) and lower crystallite size and large surface area which was ensured by DRS, XRD, and FESEM analyses, respectively. The degradation rate of the catalyst was constructed from pseudo-first-order kinetics (Figure 7(c)). The kinetic equation is as follows: $-\ln(C_t/C_0) = -Kt$, where C_t is the light irradiated dye absorbance at time t , C_0 is the initial dye absorbance at time $t = 0$, and t is the activity time of degradation. The obtained pseudo-first-order kinetics delivered the ultraviolet irradiation potential which is more effective than visible light irradiation. The present work is compared with earlier published work of TiO₂ nanoparticles. The comparison of TiO₂ nanoparticle photocatalytic activity is tabulated in Table 1. The pure and doped TiO₂ photocatalytic degradation work is reported. The degradation is based on the light source, size, dopants, and surface area. The table denotes the catalytic activity of TiO₂ nanoparticles in various doping, light sources, and time. The visible light irradiation degradation is low compared to ultraviolet irradiation but the addition of metal compounds increased the catalytic efficiency. Free radicals production increased the oxidation ability of dye molecules. The radical formations are evoked in visible light irradiation [64–67]. The present visible light irradiation catalytic activity produced the superoxides and radicals which exhibited a better photocatalytic dye degrada-

tion activity than previously reported works. Therefore, the present work focused on visible and ultraviolet light irradiation and demonstrates that biogenic TiO₂ nanoparticles prove heightened degradation ability against the MB dye.

The photocatalyst mechanism of the TiO₂ nanoparticles is shown in Figure 8. The mechanism of TiO₂ nanoparticle-excited electrons traveled from the valence band to the conduction band during the illumination. The modified electrons and holes get a reduction and oxidation property. The generated charge carriers produce free radicals and superoxides. These compounds dissociated the dye molecules to noxious compounds [61, 62, 68, 69]. The UV light irradiation inhibits the e-h pair very strappingly and produces an enormous amount of free radicals than visible light irradiation. The detailed mechanism is as follows:



Based on the results, specify that the green synthesized TiO₂ nanoparticles have upgraded catalytic activity and enhanced dye adsorption behavior in ultraviolet light irradiation. Hence, the green synthesized TiO₂ nanoparticles detached the dye molecules from the aquatic surface and more powerful degradation in the ultraviolet region.

4. Conclusion

The current work reported the green production of nanoparticles from *Phyllanthus niruri* leaf extract. The plant extract using nanoparticles is an eco-friendly and noxious-free reduction to synthesize the nanophase materials. The photocatalyst of the TiO₂ structural tetragonal pattern was confirmed by XRD, and their size 23 nm was calculated using the Debye Scherrer equation. The plant derivatives and their reduction/stabilization involved biomolecules, and their functional groups were identified from FTIR spectroscopy.

The optical measurement and their wide bandgap values were evident by DRS analysis. The spherical surface and elemental investigation were obtained from FESEM with EDX. The photocatalyst of TiO₂ nanoparticles was performed in ultraviolet and visible light irradiation against MB dye. The results exposed that ultraviolet irradiation of TiO₂ nanoparticles exhibited better catalytic activity than visible light photocatalytic activity. Therefore, constructed on the results of the current study, we recommended that the green synthesized TiO₂ nanoparticles are a more active and high possible catalyst in wastewater removal treatment.

Data Availability

All research data used to assist the findings of this work are included within the manuscript.

Conflicts of Interest

The authors have no conflict of interests.

Acknowledgments

The authors are grateful to the researchers supporting project no. (RSP-2021/326), King Saud University, Riyadh, Saudi Arabia.

References

- [1] D. Mandal, M. E. Bolander, D. Mukhopadhyay, G. Sarkar, and P. Mukherjee, "The use of microorganisms for the formation of metal nanoparticles and their application," *Applied Microbiology and Biotechnology*, vol. 69, no. 5, pp. 485–492, 2006.
- [2] S. M. Yedurkar, C. B. Maurya, and P. A. Mahanwar, "Synthesis of nanoparticles by green chemistry process and their application in surface coatings: a review," *Archives of Applied Science Research*, vol. 8, no. 5, pp. 55–69, 2016.
- [3] R. Subbaiya, R. S. Lavanya, K. Selvapriya, and M. Masilamani Selvam, "Green synthesis of silver nanoparticles from *Phyllanthus Amarus* and their antibacterial and antioxidant properties," *International Journal of Current Microbiology and Applied Sciences*, vol. 3, no. 1, pp. 600–606, 2014.
- [4] E. T. Bekele, B. A. Gonfa, O. A. Zelekew, H. H. Belay, and F. K. Sabir, "Synthesis of titanium oxide nanoparticles using root extract of *kniphofia foliosa* as a template, characterization, and its application on drug resistance bacteria," *Journal of Nanomaterials*, vol. 2020, Article ID 2817037, 10 pages, 2020.
- [5] V. Helan, J. J. Prince, N. A. Al-Dhabi et al., "Neem leaves mediated preparation of NiO nanoparticles and its magnetization, coercivity and antibacterial analysis," *Results in Physics*, vol. 6, pp. 712–718, 2016.
- [6] I. Hussain, N. B. Singh, A. Singh, H. Singh, and S. C. Singh, "Green synthesis of nanoparticles and its potential application," *Biotechnology Letters*, vol. 38, no. 4, pp. 545–560, 2016.
- [7] B. E. Azar, A. Ramazani, S. T. Fardood, and A. Morsali, "Green synthesis and characterization of ZnAl₂O₄@ZnO nanocomposite and its environmental applications in rapid dye degradation," *Optik*, vol. 208, article 164129, 2020.
- [8] S. TaghaviFardood, A. Ramazani, F. Moradnia, Z. Afshari, S. Ganjkanlu, and F. YekkeZare, "Green synthesis of ZnO nanoparticles via sol-gel method and investigation of its application in solvent-free synthesis of 12-aryl-tetrahydrobenzo[*a*]xanthene-11-one derivatives under microwave irradiation," *Chemical Methodologies*, vol. 3, no. 6, pp. 696–706, 2019.
- [9] S. TaghaviFardood, F. Moradnia, S. Moradi, R. Forootan, F. YekkeZare, and M. Heidari, "Eco-friendly synthesis and characterization of α -Fe₂O₃ nanoparticles and study of their photocatalytic activity for degradation of Congo red dye," *Nanochemistry Research*, vol. 4, no. 2, pp. 140–147, 2019.
- [10] C. R. Resmi, P. Sreejamol, and P. Pillai, "Green synthesis of silver nanoparticles using *Azadirachta indica* leaves extract and evaluation of antibacterial activities," *International Journal of Advanced Biotechnology and Research*, vol. 4, pp. 300–303, 2014.
- [11] A. Thirumurugan, P. Aswitha, C. Kiruthika, S. Nagarajan, and A. N. Christy, "Green synthesis of platinum nanoparticles using *Azadirachta indica*-an eco-friendly approach," *Materials Letters*, vol. 170, pp. 175–178, 2016.
- [12] S. Dewanjee, M. Kundu, A. Maiti, R. Majumdar, A. Majumdar, and S. C. Mandal, "In vitro evaluation of antimicrobial activity of crude extract from plants *Diospyros peregrina*, *Coccinia grandis* and *Swietenia macrophylla* trop," *Journal of Pharmacy Research*, vol. 6, p. 773, 2007.
- [13] A. K. Bhattacharjee and A. K. Das, "Phytochemical survey of few Mysore plants," *Economic Botany*, vol. 23, no. 3, pp. 274–276, 1969.
- [14] K. S. Landage, G. K. Arbade, P. Khanna, and C. J. Bhongale, "Biological approach to synthesize TiO₂ nanoparticles using *Staphylococcus aureus* for antibacterial and anti-biofilm applications," *Journal of Microbiology & Experimentation*, vol. 8, no. 1, pp. 36–43, 2020.
- [15] I. Halomoan, Y. Yulizar, R. M. Surya, and D. O. B. Apriandanu, "Facile preparation of CuO-Gd₂Ti₂O₇ using *Acmella uliginosa* leaf extract for photocatalytic degradation of malachite green," *Materials Research Bulletin*, vol. 150, article 111726, 2022.
- [16] Y. Yulizar, D. O. B. Apriandanu, and R. M. Surya, "Fabrication of novel SnWO₄/ZnO using *Muntingia calabura* L. leaf extract with enhanced photocatalytic methylene blue degradation under visible light irradiation," *Ceramics International*, vol. 48, no. 3, pp. 3564–3577, 2022.
- [17] A. Indriyani, Y. Yulizar, R. T. Yunarti, D. O. B. Apriandanu, and R. M. Surya, "One-pot green fabrication of BiFeO₃ nanoparticles via *Abelmoschus esculentus* L leaves extracts for photocatalytic dye degradation," *Applied Surface Science*, vol. 563, article 150113, 2021.
- [18] Y. Yulizar, J. Gunlazuardi, D. O. B. Apriandanu, and T. W. W. Syahfitri, "CuO-modified CoTiO₃ via *Catharanthus roseus* extract: A novel nanocomposite with high photocatalytic activity," *Materials Letters*, vol. 277, article 128349, 2020.
- [19] Y. Yulizar, D. O. B. Apriandanu, and F. L. Hakim, "Two-phase synthesis in n-hexane–water, characterization, and photocatalytic activity of ZnO/Bi₂Sn₂O₇ nanocomposite," *JOM*, vol. 73, no. 1, pp. 441–449, 2021.
- [20] Y. Yulizar, A. Eprasatya, D. O. B. Apriandanu, and R. T. Yunarti, "Facile synthesis of ZnO/GdCo₃ nanocomposites, characterization and their photocatalytic activity under visible light illumination," *Vacuum*, vol. 183, article 109821, 2021.
- [21] Y. Yulizar, D. O. B. Apriandanu, and A. P. Wibowo, "Plant extract mediated synthesis of Au/TiO₂ nanocomposite and its photocatalytic activity under sodium light irradiation," *Composites Communications*, vol. 16, pp. 50–56, 2019.

- [22] Y. Yulizar, D. O. B. Apriandanu, and R. I. Ashna, "La₂CuO₄-decorated ZnO nanoparticles with improved photocatalytic activity for malachite green degradation," *Chemical Physics Letters*, vol. 755, article 137749, 2020.
- [23] Y. Yulizar, E. Kusriani, D. O. B. Apriandanu, and N. Nurdini, "Datura metel L. leaves extract mediated CeO₂ nanoparticles: synthesis, characterizations, and degradation activity of DPPH radical," *Surfaces and Interfaces*, vol. 19, article 100437, 2020.
- [24] J. Abdul, S. Salman, K. H. Ibrahim, and F. A. Ali, "Effect of culture media on biosynthesis of titanium dioxide nanoparticles using *Lactobacillus crispatus* material and methods: results and discussion," *International Journal of Advanced Research*, vol. 2, no. 5, pp. 1014–1021, 2014.
- [25] C. Jayaseelan, A. A. Rahuman, S. M. Roopan et al., "Biological approach to synthesize TiO₂ nanoparticles using *Aeromonas hydrophila* and its antibacterial activity," *Spectrochimica Acta Part A: Molecular and Biomolecular Spectroscopy*, vol. 107, pp. 82–89, 2013.
- [26] R. Joerger, T. Klaus, and C. G. Granqvist, "Biologically produced silver-carbon composite materials for optically functional thin-film coatings," *Advanced Materials*, vol. 12, no. 6, pp. 407–409, 2000.
- [27] W. M. Tolles and B. B. Rath, "Nanotechnology, a stimulus for innovation," *Current Science*, vol. 85, no. 12, pp. 1746–1759, 2003.
- [28] A. Vishnu Kirthi, A. Abdul Rahuman, G. Rajakumar et al., "Biosynthesis of titanium dioxide nanoparticles using bacterium *Bacillus subtilis*," *Materials Letters*, vol. 65, no. 17–18, pp. 2745–2747, 2011.
- [29] C. Gélis, S. Girard, A. Mavon, M. Delverdier, N. Paillous, and P. Vicendo, "Assessment of the skin photoprotective capacities of an organo-mineral broad-spectrum sunblock on two ex vivo skin models," *Photodermatology, Photoimmunology & Photomedicine*, vol. 19, no. 5, pp. 242–253, 2003.
- [30] S. Hussain, X. Yang, M. K. Aslam et al., "Robust TiN nanoparticles polysulfide anchor for Li-S storage and diffusion pathways using first principle calculations," *Chemical Engineering Journal*, vol. 391, article 123595, 2020.
- [31] S. Hussain, A. J. Khan, M. Arshad et al., "Charge storage in binder-free 2D-hexagonal CoMoO₄ nanosheets as a redox active material for pseudocapacitors," *Ceramics International*, vol. 47, no. 6, pp. 8659–8667, 2021.
- [32] S. Hussain, M. Hassan, M. S. Javed et al., "Distinctive flower-like CoNi₂S₄ nanoneedle arrays (CNS-NAs) for superior supercapacitor electrode performances," *Ceramics International*, vol. 46, no. 16, pp. 25942–25948, 2020.
- [33] S. Hussain, N. Ullah, Y. Zhang et al., "One-step synthesis of unique catalyst Ni₉S₈@C for excellent MOR performances," *International Journal of Hydrogen Energy*, vol. 44, no. 45, pp. 24525–24533, 2019.
- [34] S. Hussain, M. S. Javed, S. Asim et al., "Novel gravel-like NiMoO₄ nanoparticles on carbon cloth for outstanding supercapacitor applications," *Ceramics International*, vol. 46, no. 5, pp. 6406–6412, 2020.
- [35] D. K. Ved and G. S. Goraya, *A Text Book of Demand and Supply of Medicinal Plants in India*, NMPB, New Delhi and FRLHT, Bangalore, India, 2008.
- [36] D. W. Unander, G. L. Webster, and B. S. Blumberg, "Usage and bioassays in *Phyllanthus* (Euphorbiaceae). IV. Clustering of antiviral uses and other effects," *Journal of Ethno-Pharmacology*, vol. 45, no. 1, pp. 1–18, 1995.
- [37] G. L. Webster, "Classification of the Euphorbiaceae," *Annals of the Missouri Botanical Garden*, vol. 81, no. 1, pp. 3–32, 1994.
- [38] B. Joseph and S. J. Raj, "An overview: pharmacognostic Properties of *Phyllanthus amarus* Linn," *International Journal of Pharmacology*, vol. 7, no. 1, pp. 40–45, 2010.
- [39] G. Ravikant, R. Srirama, U. Senthilkumar, K. N. Ganeshaiyah, and R. Umashaanker, "Genetic Resources of *Phyllanthus* in Southern India: Identification of Geographic and Genetic Hot Spots and Its Implication for Conservation," in *Phyllanthus Species, Scientific Evaluation and Medicinal Applications*, pp. 97–118, CRC Press, 2011.
- [40] A. K. Khanna, F. Rizvi, and R. Chander, "Lipid lowering activity of *Phyllanthus niruri* in hyperlipemic rats," *Journal of Ethnopharmacology*, vol. 82, no. 1, pp. 19–22, 2002.
- [41] J. Meena, R. A. Sharma, and R. Rolania, "A review on phytochemical and pharmacological properties of *Phyllanthus amarus* Schum. and Thonn," *International Journal of Pharmaceutical Sciences and Research*, vol. 9, no. 4, pp. 1377–1386, 2018.
- [42] K. Narendra, J. Swathi, K. M. Sowjanya, and A. Krishna Satya, "Phyllanthus niruri: a review on its ethno botanical, phytochemical and pharmacological profile," *Journal of Pharmacy Research*, vol. 5, no. 9, pp. 4681–4691, 2012.
- [43] S. Shanavas, A. Priyadharsan, S. Karthikeyan et al., "Green synthesis of titanium dioxide nanoparticles using *Phyllanthus niruri* leaf extract and study on its structural, optical and morphological properties," *Materials Today: Proceedings*, vol. 26, pp. 3531–3534, 2020.
- [44] A. Panneerselvam, J. Velayutham, and S. Ramasamy, "Green synthesis of TiO₂ nanoparticles prepared from *Phyllanthus niruri* leaf extract for dye adsorption and their isotherm and kinetic studies," *IET Nanobiotechnology*, vol. 15, no. 2, pp. 164–172, 2021.
- [45] M. Sathish Kumar, M. Saroja, and M. Venkatachalam, "Characterization and antimicrobial activity of green synthesized zinc sulphide nanoparticles using plant extracts of *Phyllanthus niruri*," *International Journal of Chemical Sciences*, vol. 15, no. 2, pp. 123–130, 2017.
- [46] K. Singh, M. Panghal, S. Kadyan, U. Chaudhary, and J. P. Yadav, "Green silver nanoparticles of *Phyllanthus amarus*: as an antibacterial agent against multi drug resistant clinical isolates of *Pseudomonas aeruginosa*," *Journal of Nanobiotechnology*, vol. 12, no. 1, p. 40, 2014.
- [47] W. W. Andualem, F. K. Sabir, E. T. Mohammed, H. H. Belay, and B. A. Gonfa, "Synthesis of copper oxide nanoparticles using plant leaf extract of *Catha edulis* and its antibacterial activity," *Journal of Nanotechnology*, vol. 2020, Article ID 2932434, 10 pages, 2020.
- [48] M. D. Purkayastha, T. P. Majumder, M. Sarkar, and S. Ghosh, "Carrier Transport and Shielding Properties of Rod-Like Mesoporous TiO₂-SiO₂ Nanocomposite," *Radiation Physics and Chemistry*, vol. 192, article 109898, 2021.
- [49] Y. Huang, J. Liang, M. Xu et al., "Stereotaxically constructed graphene modification of CuO-Cu₂O/TiO₂ microspheres for boosted lithium and sodium storage performance," *Journal of Electronic Materials*, vol. 51, no. 1, pp. 47–56, 2021.
- [50] A. Chinnathambi, S. Vasantharaj, M. Saravanan et al., "Bio-synthesis of TiO₂ nanoparticles by *Acalypha indica*; photocatalytic degradation of methylene blue," *Applied Nanoscience*, vol. 11, pp. 1–8, 2021.

- [51] S. S. Bahri, Z. Harun, S. K. Hubadillah et al., "Review on recent advance biosynthesis of TiO₂nanoparticles from plant-mediated materials: characterization, mechanism and application," *IOP Conference Series: Materials Science and Engineering*, vol. 1142, no. 1, article 012005, 2021.
- [52] M. Saleem, M. Y. Naz, S. Shukrullah, S. Ali, and S. T. A. Hamdani, "Ultrasonic biosynthesis of TiO₂ nanoparticles for improved self-cleaning and wettability coating of DBD plasma pre-treated cotton fabric," *Applied Physics A*, vol. 127, no. 8, 2021.
- [53] R. Aswini, S. Murugesan, and K. Kannan, "Bio-engineered TiO₂nanoparticles usingLedebouria revolutaextract: larvicidal, histopathological, antibacterial and anticancer activity," *International Journal of Environmental Analytical Chemistry*, vol. 101, no. 15, pp. 2926–2936, 2021.
- [54] A. Fall, I. Ngom, M. Bakayoko et al., "Biosynthesis of TiO₂ nanoparticles by using natural extract of Citrus sinensis," *Materials Today: Proceedings*, vol. 36, pp. 349–356, 2021.
- [55] K. Lingaraju, R. B. Basavaraj, K. Jayanna et al., "Biocompatible fabrication of TiO₂ nanoparticles: antimicrobial, anticoagulant, antiplatelet, direct hemolytic and cytotoxicity properties," *Inorganic Chemistry Communications*, vol. 127, article 108505, 2021.
- [56] M. K. Singh and M. S. Mehata, "Temperature-dependent photoluminescence and decay times of different phases of grown TiO₂ nanoparticles: carrier dynamics and trap states," *Ceramics International*, vol. 47, no. 23, pp. 32534–32544, 2021.
- [57] L. Zhou, Z. Shen, S. Wang et al., "Construction of quantum-scale catalytic regions on anatase TiO₂ nanoparticles by loading TiO₂ quantum dots for the photocatalytic degradation of VOCs," *Ceramics International*, vol. 47, no. 15, pp. 21090–21098, 2021.
- [58] G. Nabi, A. Majid, A. Riaz, T. Alharbi, M. A. Kamran, and M. Al-Habardi, "Green synthesis of spherical TiO₂ nanoparticles using Citrus limetta extract: excellent photocatalytic water decontamination agent for RhB dye," *Inorganic Chemistry Communications*, vol. 129, article 108618, 2021.
- [59] K. S. Khashan, G. M. Sulaiman, F. A. Abdulameer et al., "Antibacterial activity of TiO₂ nanoparticles prepared by one-step laser ablation in liquid," *Applied Sciences*, vol. 11, no. 10, p. 4623, 2021.
- [60] K. Mallikarjuna, S. V. P. Vattikuti, R. Manne et al., "Sonochemical synthesis of silver quantum dots immobilized on exfoliated graphitic carbon nitride nanostructures using ginseng extract for photocatalytic hydrogen evolution, dye degradation, and antimicrobial studies," *Nanomaterials*, vol. 11, no. 11, p. 2918, 2021.
- [61] K. N. Pandiyaraj, D. Vasu, R. Ghobeira et al., "Dye wastewater degradation by the synergetic effect of an atmospheric pressure plasma treatment and the photocatalytic activity of plasma-functionalized Cu–TiO₂ nanoparticles," *Journal of Hazardous Materials*, vol. 405, article 124264, 2021.
- [62] J. Singh, S. Juneja, R. K. Soni, and J. Bhattacharya, "Sunlight mediated enhanced photocatalytic activity of TiO₂ nanoparticles functionalized CuO- Cu₂O nanorods for removal of methylene blue and oxytetracycline hydrochloride," *Journal of Colloid and Interface Science*, vol. 590, pp. 60–71, 2021.
- [63] S. Sagadevan, J. A. Lett, G. K. Weldegebrieal et al., "Enhanced gas sensing and photocatalytic activity of reduced graphene oxide loaded TiO₂ nanoparticles," *Chemical Physics Letters*, vol. 780, article 138897, 2021.
- [64] P. Monazzam and B. F. Kisomi, "Co/TiO₂ Nanoparticles: Preparation, Characterization and Its Application for Photocatalytic Degradation of Methylene Blue," *Desalination and Water Treatment*, vol. 63, pp. 283–292, 2017.
- [65] R. Chauhan, A. Kumar, and R. P. Chaudhary, "Structural and photocatalytic studies of Mn doped TiO₂ nanoparticles," *Spectrochimica Acta Part A: Molecular and Biomolecular Spectroscopy*, vol. 98, pp. 256–264, 2012.
- [66] L. Gnanasekaran, R. Hemamalini, R. Saravanan, K. Ravichandran, F. Gracia, and V. K. Gupta, "Intermediate state created by dopant ions (Mn, Co and Zr) into TiO₂ nanoparticles for degradation of dyes under visible light," *Journal of Molecular Liquids*, vol. 223, pp. 652–659, 2016.
- [67] P. Karuppasamy, N. R. N. Nisha, A. Pugazhendhi, S. Kandasamy, and S. Pitchaimuthu, "An investigation of transition metal doped TiO₂ photocatalysts for the enhanced photocatalytic decoloration of methylene blue dye under visible light irradiation," *Journal of Environmental Chemical Engineering*, vol. 9, no. 4, article 105254, 2021.
- [68] M. R. Bindhu, T. D. Willington, M. R. Hatshan, S. M. Chen, and T. W. Chen, "Environmental photochemistry with Sn/F simultaneously doped TiO₂ nanoparticles: UV and visible light induced degradation of thiazine dye," *Environmental Research*, vol. 207, article 112108, 2021.
- [69] E. T. Helmy, E. M. Abouellef, U. A. Soliman, and J. H. Pan, "Novel green synthesis of S-doped TiO₂ nanoparticles using *Malva parviflora* plant extract and their photocatalytic, antimicrobial and antioxidant activities under sunlight illumination," *Chemosphere*, vol. 271, article 129524, 2021.
- [70] M. Aravind, M. Amalanathan, and M. Mary, "Synthesis of TiO₂ nanoparticles by chemical and green synthesis methods and their multifaceted properties," *SN Applied Sciences*, vol. 3, no. 4, pp. 1–10, 2021.
- [71] D. Achudhan, S. Vijayakumar, B. Malaikozhundan et al., "The antibacterial, antibiofilm, antifogging and mosquitocidal activities of titanium dioxide (TiO₂) nanoparticles green-synthesized using multiple plants extracts," *Journal of Environmental Chemical Engineering*, vol. 8, no. 6, article 104521, 2020.
- [72] R. J. Barnes, R. Molina, J. Xu, P. J. Dobson, and I. P. Thompson, "Comparison of TiO₂ and ZnO nanoparticles for photocatalytic degradation of methylene blue and the correlated inactivation of gram-positive and gram-negative bacteria," *Journal of Nanoparticle Research*, vol. 15, no. 2, 2013.
- [73] K. S. Saranya, V. V. T. Padil, C. Senan et al., "Green synthesis of high temperature stable anatase titanium dioxide nanoparticles using gum kondagogu: characterization and solar driven photocatalytic degradation of organic dye," *Nanomaterials*, vol. 8, no. 12, p. 1002, 2018.
- [74] S. A. Yasin, J. A. Abbas, M. M. Ali, I. A. Saeed, and I. H. Ahmed, "Methylene blue photocatalytic degradation by TiO₂ nanoparticles supported on PET nanofibres," *Materials Today: Proceedings*, vol. 20, pp. 482–487, 2020.